The effect of defect field on dielectric ageing of lead magnesium niobate-lead titanate relaxor ferroelectrics

2000 J. Phys.: Condens. Matter 12 4381

(http://iopscience.iop.org/0953-8984/12/19/308)

J. Phys.: Condens. Matter **12** (2000) 4381–4390. Printed in the UK PII: S0953-8984(00)06114-2

The effect of defect field on dielectric ageing of lead magnesium niobate–lead titanate relaxor ferroelectrics

Huiqing Fan†§, Litong Zhang†, Liangying Zhang‡ and Xi Yao‡

† State Key Laboratory of Solidification Processing, Northwestern Polytechnical University, Xi'an 710072, People's Republic of China

‡ Electronic Materials Research Laboratory, Xi'an Jiaotong University, Xi'an 710049, People's Republic of China

E-mail: hqfan2@yahoo.com

Received 19 July 1999, in final form 28 January 2000

Abstract. The ageing effect on the temperature dependence of the dielectric permittivity and loss angle tangent was examined for $Pb(Mg_{1/3}Nb_{2/3})_{0.9}Ti_{0.1}O_3$ and 0.1 wt% MnO–$Pb(Mg_{1/3}Nb_{2/3})_{0.95}Ti_{0.05}O_3$ ceramics. A Debye-like dielectric relaxation process was clearly observed in the higher temperature range for the latter composition, but not for the former. It is stressed that the metastability of the ferroelectric domain structure is due to the presence of defect dipoles in perovskites. Compared with the dielectric poling behaviour of the compositions, a pin effect was introduced to analyse the differences and similarities of reorientation and alignment of microdomain with macrodomain. Defect dipoles are formed from pairs of vacancy and positively charged dopant sites and they provide pinning centres to ferroelectric microdomain walls. As a consequence, microdomains re-establish along a certain direction over time, and the microstructure changes from a disordering to an apparent ordering. Thus a perovskite relaxor ferroelectrics with acceptor dopants exhibits a significant time dependent decrease in the complex dielectric response.

1. Introduction

Perovskite relaxor ferroelectrics are a special class for ferroelectric materials, which is characterized by broad maximum of weak-field dielectric permittivity [1] and its frequency-dependent behaviour. For a normal ferroelectric material, there is no significant frequency dispersion at the ferroelectric–paraelectric phase transition region at radio frequencies (sub-GHz). However, for relaxor ferroelectrics, a strong frequency dispersion exists at the so-called diffused phase transition region, and the structure also remains pseudocubic without macroscopic polarization even at temperatures near 0 K. In fact, overwhelming experimental evidence from the thermal expansion, optical refractive index, and x-ray diffraction experiments has shown that local polarization microdomains exist in nanoscale, which may be a key to the understanding of the behaviour of relaxor ferroelectrics [2–6].

Field-induced and zero-field micro–macrodomain transitions have been thoroughly investigated by Chu *et al* [7] and Dai *et al* [8]. These studies clearly revealed how the dielectric behaviour changes from that of typical relaxor ferroelectrics to that of typical normal ferroelectrics. Relaxor ferroelectrics corresponds to the ferroelectric microdomain state. When ferroelectric macrodomains are formed, the weakness of dielectric dispersion will be observed. Otherwise, ageing of relaxor ferroelectrics can distort the temperature response of dielectric

§ Author to whom all correspondence should be addressed.

0953-8984/00/194381+10$30.00

dispersion, and dielectric dispersion also becomes weak above the ageing temperature [9, 10]. This type of weakness of dielectric dispersion is always attributed to the reorientation and alignment of microdomain in materials. Therefore, the purpose of the present work is to discuss the re-establishment of microstructure in process of time and the relationships between the macrodomain and the reoriented microdomain in relaxor ferroelectrics.

The complex dielectric responses of $Pb(Mg_{1/3}Nb_{2/3})_{0.9}Ti_{0.1}O_3$ (PMNT1) and 0.1 wt% MnO–$Pb(Mg_{1/3}\ Nb_{2/3})_{0.95}Ti_{0.05}O_3$ (PMNT2) ceramics have been carefully investigated in a temperature range from −150 to 450 °C. Distinct evidence of the compositions has been discovered for the former and the latter, which can be related to their ageing phenomenon in thermal cycle measurements. After comparing their dielectric poling behaviours and their electric hysteresis loops, we found that the pinning effect can explain all the results very well.

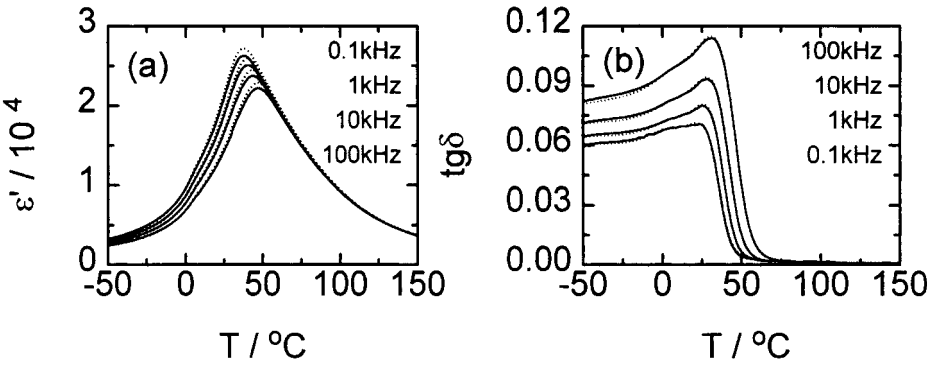

Figure 1. Temperature dependence of the dielectric permittivity (a) and loss angle tangent (b) for fresh (· · · · · ·) and aged (——) PMNT1 ceramics.

2. Experimental procedures

For the preparation of PMNT1 and PMNT2 ceramics, a two-step method was used [11]. The starting chemical materials were PbO, MgO, Nb_2O_5, TiO_2 and MnO (99.9% purity). In the processing, MgO and Nb_2O_5 were first reacted in a precalcine to form the columbite structure $MgNb_2O_6$ for 2 h at 900 °C. For doping, the MnO was introduced using a dilute solution of $Mn(NO_3)_2$ added to the calcine together with $MgNb_2O_6$, PbO and TiO_2. The chemicals were weighed and ball milled for 24 h with ZrO_2 media and alcohol. Pellets of mixed powder pressed under a low pressure were calcined for 2 h at 800 °C. The calcined pellets were then cracked and mixed with ZrO_2 media and alcohol by planetary milling. The dried mixture was then pelletized under 10 MPa pressure and sintered with $PbZrO_3$ atmospheric powders in a covered crucible at 1100 °C for 2 h. The final sintered samples were all about 97% of the theoretical density and shown by x-ray diffraction to be free from contamination by the pyrochlore phase. With regards to dielectric measurement, samples of a disc shape with a thickness about 1 mm and a diameter of about 10 mm were used. Gold electrodes were deposited on the ground parallel sample surfaces by dc sputtering.

The weak-field dielectric response was measured by using a Hewlett Packard 4274A LCR meter. Samples were placed in a test chamber, which can be operated between −196 and 200 °C. The four-terminal pair configuration, which was connected together directly to electrodes of the sample, was used to increase the measuring accuracy. Before the

measurement, a standard calibration was performed to remove any stray capacitance and lead and contact resistance. The temperature was measured using a Hewlett Packard 3455A digital volt-meter via a platinum resistance thermometer mounted directly on the ground electrode of the sample fixture. The amplitude level of the signal was 5 V cm^{-1}. The temperature controllers, HP3455A and HP4274A, were controlled with a personal computer. The high-temperature dielectric data was obtained by putting the sample in a small furnace specifically equipped for such measurements. Data was taken by cooling the sample from high temperature ($\sim$500 °C) to room temperature at a rate of 1 °C min^{-1}.

Samples were aged under open-circuit conditions at a 15–20 °C room temperature for one year; then the temperature was lowered to −180 °C, and the sample was measured during heating at a rate of 1 °C min^{-1}. The ageing temperature (T_a) was set around 20 °C, several degrees lower than the temperature of the dielectric permittivity maximum (T_m) of samples, in order that the relatively strong ageing could be tested. When poling is required, the sample was poled by applying a dc electric field of 20 kV cm^{-1} at 200 °C for 15 min and cooled to −180 °C under the electric field. After removing the field, and shorting the electrodes for 10 min to release the surface charge, dielectric response measurements were made on heating at a rate of 1 °C min^{-1}. Samples were heated to 200 °C for 1 h to refresh the previous ageing and poling, and then the structure and properties for fresh samples were tested.

The ferroelectric hysteresis loop (P–E) was characterized by using a computer-controlled, modified Sawyer–Tower circuit. A 1 Hz sine wave voltage was applied to the sample by a Trek 610 high-voltage amplifier whose input signal was generated by the computer. The output signal from the sample was obtained and processed by the computer.

A Rigaku DMAX-3 x-ray diffractometer was used to analyse the phase structure of samples employing Cu Kα radiation. Ceramic pellets with ground and polished surfaces were studied.

In order to examine the domain structure, thin foils were prepared by standard ceramographic techniques using a Gatan 'dual-ion mill' (model 600) operated at 5 kV with a combined gun current of 1 mA. The foils were investigated by transmission electron microscopy (TEM) using a JEOL JEM-200 CX transmission electron microscope.

3. Results and discussion

The temperature dependence of the dielectric response for PMNT1 is shown in figure 1. As shown in the figure, there is a very weak ageing within the temperature range for the PMNT1. Figure 2 shows the typical dielectric response of aged and fresh PMNT2. The curve may be divided into four regions, all of which coincide with the results of the earlier ageing studies on doped and undoped PMNT1 specimens [12]. At higher temperatures, we also observed an increase in the dielectric loss angle tangent for PMNT2 composition, which has been neglected by other researchers, so we carefully carried out a detailed study on this phenomenon.

Figure 3 exhibits the detailed effect of the dielectric loss angle tangent for the PMNT1 and PMNT2 compositions. It can be clearly seen that there is a Debye-like dielectric relaxation process in the higher temperature range for the latter composition, but not for the former. The frequency dependence of the temperature of the dielectric loss angle tangent maximum (T'_{max}) in this temperature range obeys the Arrhenius law

$$\omega = \omega_0 \exp(-T_0/T'_{max}) \tag{1}$$

where ω_0 is the attempt frequency of the dipole molecule, $T_0 = E_a/k$, E_a is the activation energy for dipole relaxation and k is Boltzmann's constant. The $1/T'_{max}$ as a function of measurement frequency is shown in figure 4. The value of the activation energy E_a (0.718 eV) corresponds to the dipole state for Debye relaxation [13].

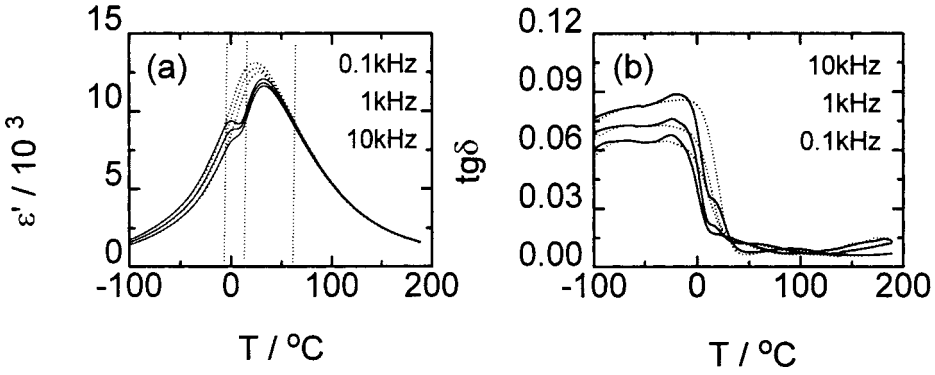

Figure 2. Temperature dependence of the dielectric permittivity (a) and loss angle tangent (b) for fresh (· · · · · ·) and aged (——) PMNT2 ceramics.

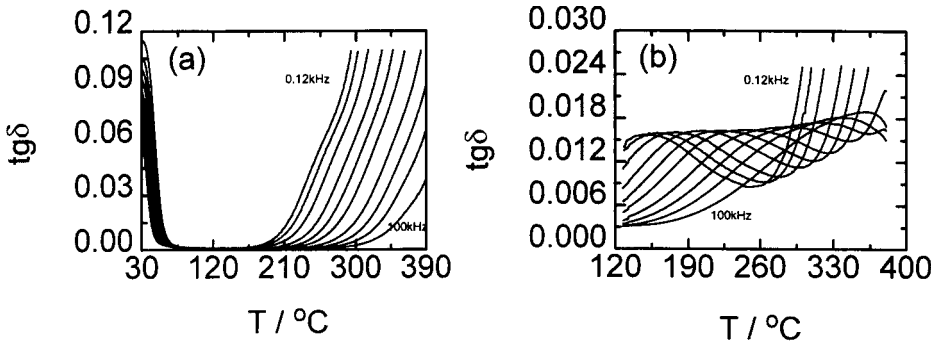

Figure 3. Temperature dependence of the dielectric loss angle tangent in the high-temperature range for PMNT1 (a) and PMNT2 (b) ceramics. The frequencies used were 0.12, 0.2, 0.4, 1, 2, 4, 10, 20, 40 and 100 kHz.

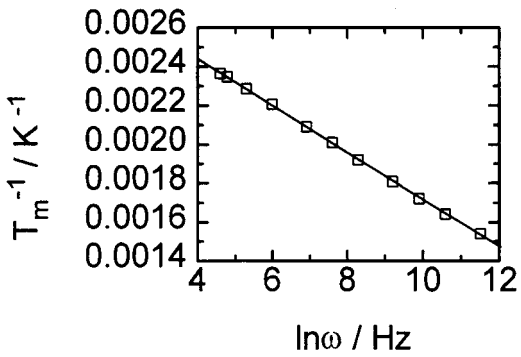

Figure 4. Experimental data (□) and fitted curve of $1/T'_{max}$ against frequency for PMNT2 ceramics.

As we know, in the undoped PMNT1 sample, the valence states of Pb, Mg, Nb, Ti and O are all equivalent valence substitutes, if the evaporation of lead in the ceramics can be neglected because of the sintering process with $PbZrO_3$ atmospheric powders in a covered crucible at high temperature. Thus, theoretically, no ageing should be observed. In practice, however, non-stoichiometricity or impurities in ceramics could not be completely avoided, so there always exists very slight ageing, shown in figure 1, that can be observed under very careful measurement.

For the PMNT2 sample, the ageing is thought to involve two parts. One part is the same as the ageing in PMNT1, and the rest is due to the Mn acceptor dopants. Mn with associated oxygen vacancies will form a defect dipole pair, and the defect bias field was shown to originate from it. The reorientation and alignment of defect dipoles with local polar microdomains provide a pinning field to micro polar regions, where the regions with larger micro polar volume will experience stronger pinning potential. Whereas the macroscopic symmetry of the relaxor ferroelectric phase is a distortion cubic, at the polar nanodomain level the symmetry is rhombohedral. Thus the structure of an aged sample should become a metastable rhombohedral phase over time. Figure 5 gives the x-ray diffraction patterns of the fresh and aged PMNT2 at room temperature, which proved the hypothesis. In particular, we can see that the relative integral intensity of the (111) reflection for the aged sample is stronger than that for the fresh sample. It also implies that locally polarized regions have a rhombohedral symmetry and, consequently, eight equivalent variants. The polarization of polar clusters in the cubic parent phase thermally fluctuates between equivalent directions. Down to T_m, the polar vector of the polar region gradually froze along one of the eight dipole orientations, thus a ferroelectric microdomain forms [14]. Depending on the type of defect existing in the specimen, it has been shown that the internal bias field developed in the ageing process can be either a volume effect (the field exists within grains and domains), or a boundary effect (it is located in the domain boundary or grain boundary).

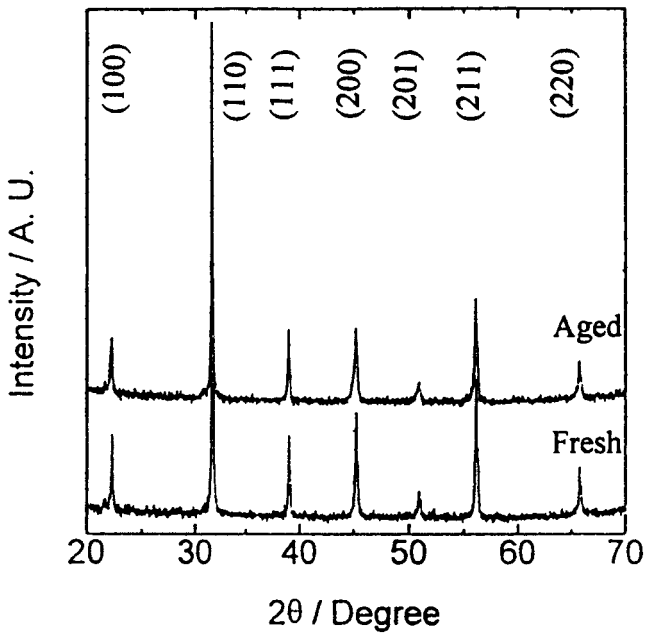

Figure 5. X-ray diffraction patterns of aged and fresh PMNT2 ceramics.

Randomly oriented polarized defects have been shown to result in double-loop-like characteristics in the P–E response. In general, the influence of polarized defects is similar to that of the homogeneous field. Consequently, the properties and phase transformation characteristics of a crystal that contains polarized defects are identical to those under application of a dc electric field or elastic strain. Figure 6 presents the polarization hysteresis loop of aged and fresh PMNT2 at room temperature. These data clearly reveal pronounced changes

depending on the electrical and thermal histories of the specimen. A very interesting double-loop-like characteristic was evident in the P–E response for the aged sample, as shown in figure 6(a). Polarization–field hysteresis loops change from a slim loop with time into a propeller shape, which indicates the re-establishment of pinned defect-domain configurations. The degree of double-loop characteristics begins to decrease as the magnitude of ac field increases, which implies that the pinning effects can be decreased and the mobility of domain boundary (microdomain walls) can be enhanced.

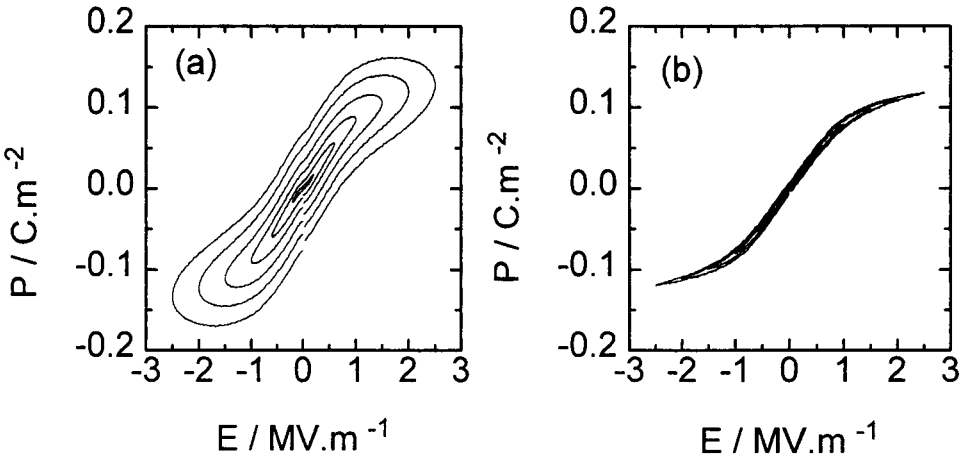

Figure 6. Evolution of P–E loops with increasing magnitude of the ac field for aged (a), fresh (b) PMNT2 ceramics.

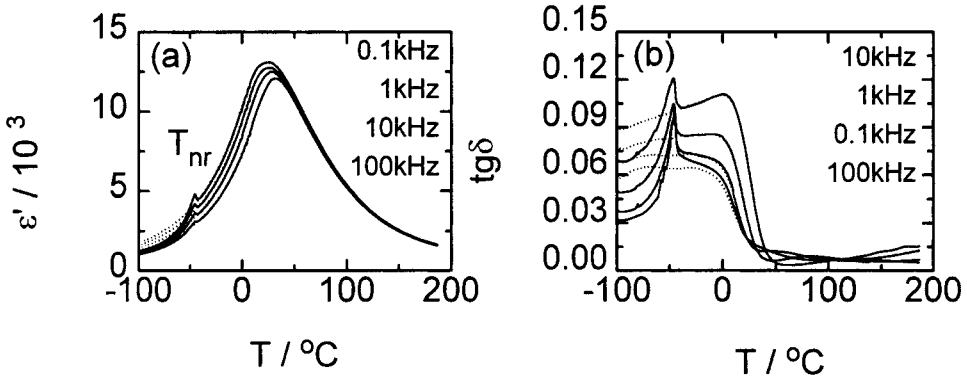

Figure 7. Temperature dependence of the dielectric permittivity (a) loss angle tangent (b) for poled (——) and fresh (· · · · · ·) PMNT2 ceramics.

Poling under dc bias possibly provides a useful way to quantify the reorientation and alignment of microdomain with macrodomain. The temperature dependence of the dielectric response of poled PMNT2 ceramics is shown in figure 7. The measurement was then made during heating with the bias field switched off. The transition temperature (T_d) from a normal to a relaxor phase becomes clearer, and does not coincide with the ageing temperature (T_a). The strong peaks of the dielectric loss angle tangent become clearer, which confirms the internal strain effect of ferroelectric micro–macrodomain switching [15]. When the sample is poled

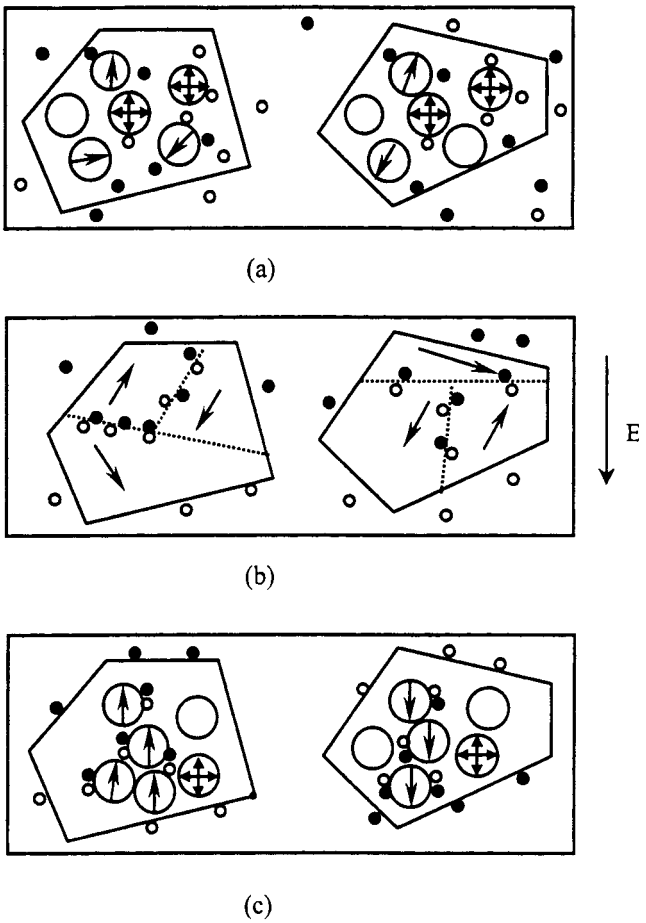

Figure 8. Distribution of defects in the sample. Exaggeration of single grains in the sample. ○ and ● denote positive and negative charged defects. The compass rose symbol denotes polar micro region and the north arrow symbol denotes a microdomain: fresh sample (a), poled sample (b) and aged sample (c).

under dc field as the temperature falls, the microdomains turn into the macrodomains shown in figure 8(b), and the macrodomains collapse into microdomains and micro polar regions again at T_d on heating. However, during ageing, the defect dipoles formed from pairs of vacancy and positively charged dopant sites provide a pinning centre to microdomain walls, thereby increasing the effective field of neighbouring microdomains. Therefore, the microdomains align along a crystallographic direction of rhombohedral symmetry within one grain, as shown in figure 8(c). The ageing occurs over long time periods near the maximum in the permittivity. This result is evidence of the reformation of nanostructures in relaxor ferroelectrics. The relaxation time of the ageing process is much longer than that of the polarization fluctuations at this temperature, indicating that there is a hierarchy of mechanisms. Defects may be able to significantly change the optimum configuration, consequently the permittivity decreases with time because the kinetics of the fluctuations and vibrations are suppressed as more favourable, and the dielectric dispersion became weak in the range of temperature above T_a because of the pinning of thermally-activated domain walls.

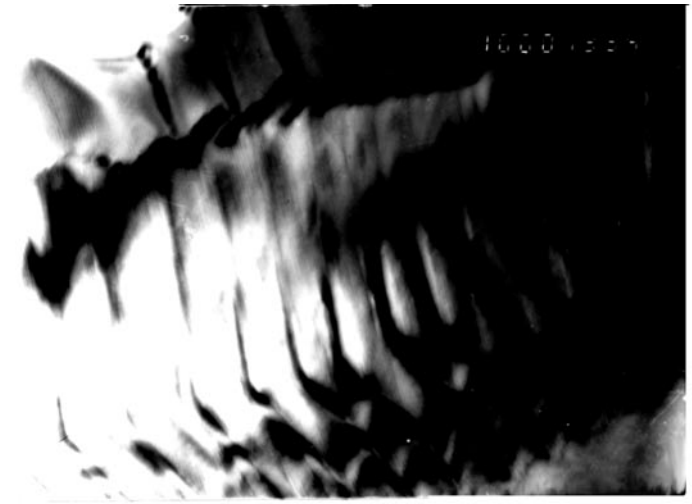

100nm (a)

100nm (b)

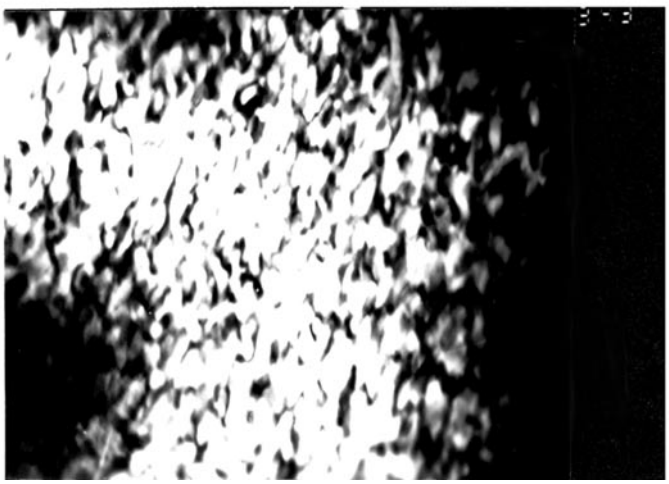

100nm (c)

Figure 9. The dark-field TEM images for aged PMNT2, $Pb(Mg_{1/3}Nb_{2/3})_{0.6}Ti_{0.4}O_3$ and PMNT1 ceramics.

Clearly, the unusual ageing behaviour of PMNT2 can be attributed to the defect field, which results in the development of complex polarized defect structures and domain boundary pinning. Thus microdomains always reorient along a special direction during ageing. Unlike most ferroelectrics where an applied electrical field only results in domain wall motion and polarization switching, in PMNT2 it results in defect redistribution and the development of internal fields. Also the thermally activated space charge in the grain boundary, free charge carriers, which is different from defect dipoles, leads to the abnormal propeller hysteresis loop as shown in figure 6(a).

Figures 9(a)–9(c) respectively show dark-field TEM images of aged PMNT2, $Pb(Mg_{1/3}Nb_{2/3})_{0.6}Ti_{0.4}O_3$ and PMNT1 specimens. Figure 9(a) reveals the presence of pinned microdomains in the aged conditions. The domains were reoriented and aligned along a certain direction. It maintained a significant degree of preferred orientation along a particular family of crystallographically-equivalent polar directions. The domain morphology is very different from the macrodomain structure that was observed in figure 9(b) for $Pb(Mg_{1/3}Nb_{2/3})_{0.6}Ti_{0.4}O_3$. In the relaxor ferroelectric state, microdomains keep disordering in figure 9(c) for PMNT1. These results clearly demonstrate that the differences and similarities of reorientation and alignment of the microdomain with the macrodomain, and the stability of microdomains, are influenced so sensitively by acceptor dopants that the dielectric ageing can be explained on the spatial distribution of defect dipoles and the defect-domain pinning configuration. Therefore, in-depth studies could provide a link between the dynamic correlation of the mesoscopic local polarization and the microscopic nature of the inner random field system.

4. Conclusions

Investigations of the influence of thermal and electrical histories on ageing of dielectric response have been performed for lead magnesium niobate–lead titanate perovskite relaxor ferroelectrics. After comparing the results of PMNT1 and PMNT2 ceramics, a Debye-like relaxation process was observed at the higher temperature range for the latter composition, and the ageing rate of it is faster than that of the former. The corresponding P–E investigations revealed double-loop characteristics that originated from a pinning effect of defects in perovskite, and the structure changes from pseudocubic to a more rhombohedral symmetry. These changes in domain stability and polarization switching mechanisms are attributed to a dependence of the spatial distribution of defect dipoles on thermal and electrical histories. The defect dipoles, formed from pairs of vacancy and positively charged dopant sites, provide a pinning centre to microdomain walls. The unusual ageing behaviour of PMNT2 can be attributed to the defect field, which results in the development of complex polarized defect structures and domain wall pinning.

Acknowledgments

The first author would like to thank Professor L F Chen, Dr Y D Xu and Dr X W Yin for their kind kelp. This research was partly supported by the Post Doctoral Science Foundation and National Natural Science Foundation of China.

References

[1] Smolensky G A 1970 *Jap. J. Phys. Soc. Suppl.* **28** 26
[2] Cross L E 1987 *Ferroelectrics* **76** 241
[3] Isupov V A 1989 *Ferroelectrics* **90** 113

[4] Bonneau P, Garnier P, Calvarin G, Husson E, Gavarri J R, Hewat A W and Morell A 1991 *J. Solid State Chem.* **91** 350
[5] Yin Z W, Chen X T, Song X Y and Feng J W 1988 *Ferroelectrics* **87** 85
[6] Yao X, Chen Z L and Cross L E 1983 *J. Appl. Phys.* **54** 3399
[7] Chu F, Setter N and Tagantsev A K 1993 *J. Appl. Phys.* **74** 5129
[8] Dai X, Xu Z and Viehland D 1994 *Phil. Mag.* B **70**33
[9] Ling H C, Yan M F and Rhodes W W 1991 *J. Am. Ceram. Soc.* **74** 287
[10] Pan W Y, Shrout T R and Cross L E 1989 *J. Mater. Sci. Lett.* **8** 771
[11] Swartz S L and Shrout T R 1982 *Mater. Res. Bull.* **17** 1245
[12] Shrout T R, Huebner W, Randall C A and Hilton A D 1989 *Ferroelectrics* **93** 361
[13] Frohlich H 1986 *Theory of Dielectrics: Dielectric Constant and Dielectric Loss* (New York: Oxford University Press)
[14] Fan H Q, Kong L B, Zhang L Y and Yao X 1999 *J. Mater. Sci.* **34** 6143
[15] Fan H Q, Kong L B, Zhang L Y and Yao X 1998 *J. Appl. Phys.* **83** 1625